



HAL
open science

Zonotopic observer designs for uncertain Takagi–Sugeno fuzzy systems

Masoud Pourasghar, Tran Anh-Tu Nguyen, Thierry-Marie Guerra

► **To cite this version:**

Masoud Pourasghar, Tran Anh-Tu Nguyen, Thierry-Marie Guerra. Zonotopic observer designs for uncertain Takagi–Sugeno fuzzy systems. *Engineering Applications of Artificial Intelligence*, 2022, 114, pp.105126. 10.1016/j.engappai.2022.105126 . hal-04278847

HAL Id: hal-04278847

<https://uphf.hal.science/hal-04278847>

Submitted on 25 Nov 2023

HAL is a multi-disciplinary open access archive for the deposit and dissemination of scientific research documents, whether they are published or not. The documents may come from teaching and research institutions in France or abroad, or from public or private research centers.

L'archive ouverte pluridisciplinaire **HAL**, est destinée au dépôt et à la diffusion de documents scientifiques de niveau recherche, publiés ou non, émanant des établissements d'enseignement et de recherche français ou étrangers, des laboratoires publics ou privés.

See discussions, stats, and author profiles for this publication at: <https://www.researchgate.net/publication/361732736>

Zonotopic Observer Designs for Uncertain Takagi–Sugeno Fuzzy Systems

Article in *Engineering Applications of Artificial Intelligence* · September 2022

DOI: 10.1016/j.engappai.2022.105126

CITATIONS

3

READS

234

3 authors:



Masoud Pourasghar

20 PUBLICATIONS 203 CITATIONS

SEE PROFILE



Anh-Tu Nguyen

Université Polytechnique Hauts-de-France

140 PUBLICATIONS 2,084 CITATIONS

SEE PROFILE



Thierry-Marie Guerra

Université Polytechnique Hauts-de-France

349 PUBLICATIONS 9,873 CITATIONS

SEE PROFILE

Zonotopic Observer Designs for Uncertain Takagi-Sugeno Fuzzy Systems

Masoud Pourasghar^a, Anh-Tu Nguyen^{a,b,*}, Thierry-Marie Guerra^a

^aUniv. Polytechnique Hauts-de-France, LAMIH CNRS UMR 8201, F-59313 Valenciennes, France

^bINSA Hauts-de-France, F-59313 Valenciennes, France

Abstract

This paper addresses the zonotopic observer design for nonlinear systems affected by uncertainties, i.e., state disturbances and measurement noises using Takagi-Sugeno (TS) fuzzy technique. The system uncertainties are considered as unknown but bounded, which are handled via a set-membership framework. For state estimation purposes, we develop an algorithm to recursively compute the zonotope containing the mismatching nonlinear term caused by unmeasured nonlinearities. Then, two methods are proposed to design the zonotopic observer gains. The first method is based on the minimization of the F -radius of zonotopes, for which the membership-function-dependent observer gain must be completely computed online. For the second method, an \mathcal{H}_∞ approach is used together with a nonquadratic Lyapunov function to determine the observer gain. Then, the zonotopic observer design is reformulated a convex optimization problem under linear matrix inequalities (LMIs), which can be effectively solved with numerical solvers. An autonomous vehicle application is provided to demonstrate and analyze the effectiveness of both proposed methods.

Keywords: Takagi-Sugeno fuzzy systems, fuzzy observers, unmeasured premise variables, state estimation, uncertainty, linear matrix inequality (LMI).

1. Introduction

Engineering systems have become increasingly complex in recent years with emerging technologies. Then, there is a surge of interest in the performance analysis of an automatic control system, as well as the examination of its safety and reliability [1]. One of the major issues in control theory is the state estimation problem, which is related to the objective of enhancing system performance and plays a crucial role in the Fault Detection (FD) of dynamical systems [2, 3]. The state estimation problem is especially difficult when dealing with nonlinear systems consisting of hundreds of constitutive elements.

In general, state estimation approaches are divided into two categories: i) model-based and ii) data-based. The former class comprises methods that utilize the mathematical model of the plant to monitor the system behaviors [3], whereas the later class mainly includes those methods using statistical methods, neural networks, fuzzy logic, etc [4]. The quality of the mathematical model is crucial for model-based methods. However, in the presence of model uncertainties, e.g., unknown disturbances and noises, there is a non-negligible mismatch between the real process behavior and its mathematical model. As a result, the influence of uncertainty and noise/disturbance is an essential factor to consider when monitoring system behavior using model-based state estimation techniques. Several approaches have been developed in the literature to explicitly include uncertainties in the mathematical model, which may be divided into

two basic paradigms: i) stochastic approaches, in which the uncertainties are represented by random variables [5, 6]; ii) deterministic approaches, in which the uncertainties are considered as unknown but bounded variables belonging to different types of sets, e.g., interval boxes, polytopes, ellipsoids, and zonotopes [7–10]. According to [11], polytopes provide tighter enclosures than interval boxes. However, the main drawback of using general polytopes is related to the complexity of vertices enumeration with respect to the space dimension. Using zonotopic representations, basic set operations can be reduced to simple matrix calculations. Despite the complexity of dealing with complex systems composed of interconnected subsystems, as well as the large number of different sensors and actuators used in these systems, employing a zonotopic set-based approach can significantly reduce the computational load for monitoring system performance. This fact has recently motivated the use of zonotopes for modeling the effect of uncertainties [12].

Most of real-world systems are with nonlinear behaviors to which the established linear system theory cannot be directly applied. Hence, various control and estimation approaches have been reported for nonlinear systems. Among these, the Takagi-Sugeno (TS) fuzzy paradigm is one of the most popular techniques to describe a large class of nonlinear systems [13–15]. First, they can be used to approximate any smooth nonlinear system with any given accuracy. In particular, using the sector nonlinearity approach, we can derive an exact TS fuzzy representation of a given nonlinear model within a compact set of the state variables. Second, thanks to its polytopic structure, TS fuzzy representation allows for some possible extensions of linear control techniques to nonlinear systems. Recent advancements have rekindled interests in monitoring the behavior

*Corresponding author.

Email addresses: mpourasg@uphf.fr (Masoud Pourasghar),
tnguyen@uphf.fr (Anh-Tu Nguyen), guerra@uphf.fr
(Thierry-Marie Guerra)

of nonlinear systems using TS fuzzy-model-based observers. TS fuzzy observers are based on TS fuzzy modeling of nonlinear systems, which are usually composed of premise variables, i.e., system nonlinearities that can be *measurable* or *unmeasurable* [16–18]. In the case of designing an TS fuzzy observer for a nonlinear system with all premise variables being measurable, the main goal will be to reduce the design conservatism by using different Lyapunov candidate functions and/or introducing slack variables [19]. In this case, the obtained results can be only applied to a limited class of TS fuzzy systems. Therefore, dealing with unmeasured premise variables in TS fuzzy observer design is essential in practice. Moreover, disturbances and/or modeling uncertainties are unavoidable in most of engineering applications. Unfortunately, the observer design for TS fuzzy systems subject to both uncertainties and unmeasured premise variables still remains open, which motivates the present work.

Furthermore, in model-based approaches, FD is based on checking/comparing the consistency of observed behavior from measured outputs utilizing sensors with anticipated behavior derived using the model [2]. This consistency test generates the residual by computing the difference between the model’s performance predicted values and the actual measured values received from the sensors [2]. The existence of fault is then detected by comparing the residual to a threshold value that takes uncertainty into account, such as parameter uncertainties, measurement noise, state disruption, etc. [20]. In practice, the existence of the defect is shown if the residual is greater than the specified threshold. Otherwise, the system is presumed to be in healthy functioning [21]. Aside from the problem of generating detection thresholds via uncertainty propagation (either using stochastic or deterministic approaches), another critical issue when using observers is determining how to compute the observer gain to be as robust as possible against the inevitable impact of uncertainties. A substantial amount of research has been reported on the examination of various methods of computing the gain to be insensitive to uncertainty, such as \mathcal{H}_∞ optimization and linear matrix inequality (LMI) based methodologies [22]. Recent studies, however, suggest that the filter design approach that simply addresses the rejection of the influence of uncertainties is useless, since the sensitivity to the fault must be included in FD filter design [23, 24]. Then, research has tended to focus on multiobjective FD design, such as $\mathcal{H}_\infty/\mathcal{H}_\infty$ [24]. Indeed, the lowest non null singular value of the transfer function matrix from fault to residual at $\omega = 0$ or over a particular frequency range accounts for the worst case of fault sensitivity [25, 26]. Then, an increasing body of research has examined this multiobjective design as an optimization problem, e.g., $\mathcal{H}_\infty/\mathcal{H}_\infty$, $\mathcal{H}_2/\mathcal{H}_2$ problems [27, 28].

The key goal of the observer design is to determine suitable observer gains such that satisfactory robustness property with respect to these effects can be achieved. Different methods have been proposed to minimize the uncertainty effects [23]. In this regard, this paper presents two methods to design zonotopic observers for uncertain TS fuzzy systems with unmeasured premise variables. For observer design, the influence of the unknown but bounded uncertainty and the mismatching

nonlinear term caused by unmeasurable nonlinearities are dealt with via a zonotopic approach, which reduces set operations to simple matrix calculations. Then, the first observer design method is based on the minimization of the F -radius of the TS fuzzy state bounding observer. For this method, the observer gain, derived from an optimality condition, is computed online. The second method is based on the use of \mathcal{H}_∞ filtering technique. Hence, the computation of the observer gain is reformulated as an optimization problem under LMI constraints. The material in this paper was partially presented [29]. The new contributions are summarized as follows.

- The technical proofs of both observer design methods are given in detail. Moreover, a nonquadratic Lyapunov function is exploited to offer more flexibility for the \mathcal{H}_∞ design method. Note that a common quadratic Lyapunov function was used in [29].
- We take into account the structure information of the unmeasured nonlinearities, considered as unknown disturbances in [29], in the observer design. To this end, a new algorithm to compute the zonotopic bounds of the mismatching nonlinear term stemmed from unmeasured nonlinearities is proposed.
- The proposed zonotopic observer designs are extended for fault detection of TS fuzzy systems. Moreover, a real-world application on nonlinear vehicle dynamics estimation and fault detection is included to illustrate the effectiveness and the usefulness of the new results.

The structure of the paper is as follows. Some preliminaries and problem formulation are given in Section 2. The zonotopic observer design and the computation of observer gain optimizing a set-based modeling for achieving the robustness against uncertainties are proposed in Section 3. In Section 4, the effectiveness of the proposed zonotopic observer designs is illustrated with an autonomous vehicle application. Finally, the conclusions are drawn in Section 5.

Notation. The set of nonnegative integers is denoted by \mathbb{Z}_+ and $\mathcal{I}_r = \{1, 2, \dots, r\} \subset \mathbb{Z}_+$. For $i \in \mathcal{I}_r$, we denote $\xi_r(i) = [0, \dots, 0, \overset{i\text{th}}{1}, 0, \dots, 0]^\top \in \mathbb{R}^r$ a vector of the canonical basis of \mathbb{R}^r . For two vectors $x, y \in \mathbb{R}^n$, the convex hull of these vectors is denoted as $\text{co}(x, y) = \{\lambda x + (1 - \lambda)y : \lambda \in [0, 1]\}$. For a matrix X , X^\top denotes its transpose, $X \succ 0$ means X is symmetric positive definite. $\text{diag}(X_1, X_2)$ denotes a block-diagonal matrix composed of X_1, X_2 . I denotes the identity matrix of appropriate dimension. In block matrices, the symbol \star stands for the terms deduced by symmetry. \oplus denotes the Minkowski sum. $\|\cdot\|_s$ denotes the s -norm, $[\underline{x}, \bar{x}]$ is an interval with lower bound \underline{x} and upper bound \bar{x} . Arguments are omitted when their meaning is clear.

2. Preliminaries and Problem Formulation

2.1. Properties of Zonotopes

We recall some useful technical materials for zonotopic observer design.

Definition 1 (Zonotope). A zonotope $\langle c_z, R_z \rangle \subset \mathbb{R}^n$ with the center $c_z \in \mathbb{R}^n$ and the generator matrix $R_z \in \mathbb{R}^{n \times p}$ is a polytopic set defined as a linear image of the unit hypercube $[-1, 1]^n$:

$$\langle c_z, R_z \rangle = \{c_z + R_z s, \quad \|s\|_\infty \leq 1\}.$$

We denote a centered zonotope as $\langle R_z \rangle = \langle 0, R_z \rangle$. Any permutation of the columns of R_z leaves it invariant.

Definition 2 (Minkowski Sum). Considering two sets \mathcal{A} and \mathcal{B} , their Minkowski sum is a set defined as

$$\mathcal{A} \oplus \mathcal{B} = \{a + b : a \in \mathcal{A}, b \in \mathcal{B}\}.$$

The Minkowski sum of two zonotopes $\mathcal{Z}_1 = \langle c_{z_1}, R_{z_1} \rangle$ and $\mathcal{Z}_2 = \langle c_{z_2}, R_{z_2} \rangle$ is defined as

$$\mathcal{Z}_1 \oplus \mathcal{Z}_2 = \langle c_{z_1} + c_{z_2}, [R_{z_1} \quad R_{z_2}] \rangle.$$

Definition 3 (Radii of Zonotopes). Let $W \in \mathbb{R}^{n \times n}$ is a positive definite matrix. The weighted Frobenius radius (F_W -radius) of the zonotope $\langle c, R \rangle \subset \mathbb{R}^n$ is the weighted Frobenius norm of R , i.e., $\|\langle c, R \rangle\|_{F,W} = \|R\|_{F,W}$. The F -radius of the zonotope $\langle c, R \rangle$ is the Frobenius norm of R , i.e., $\|\langle c, R \rangle\|_F = \|R\|_F$. Note that $\|R\|_{F,W} = \|R\|_F$ for $W = I$.

Property 1 (Linear Image). The linear image of a zonotope $\mathcal{Z} = \langle c, R \rangle$ by a compatible matrix L is $L \odot \langle c, R \rangle = \langle Lc, LR \rangle$.

Property 2 (Zonotope Inclusion [30]). Consider a family of zonotopes represented by $\mathcal{Z} = \langle c, R \rangle \subset \mathbb{R}^n$, with a vector $c \in \mathbb{R}^n$ and an interval matrix $R \in \mathbb{R}^{n \times m}$, a zonotope inclusion indicated by $\diamond(\mathcal{Z})$ is defined as

$$\diamond(\mathcal{Z}) = \langle c, [\text{mid}(R), S] \rangle,$$

where S is a diagonal matrix that satisfies

$$S_{ii} = \sum_{j=1}^m \frac{\text{diam}(R_{ij})}{2},$$

for $\forall i \in \mathcal{I}_n$, with $\text{mid}(\cdot)$ and $\text{diam}(\cdot)$ are the center and diameter of interval matrix, respectively.

Definition 4 (Interval Hull). Given a zonotope $\mathcal{Z} = \langle c, R \rangle$, the interval hull $rs(\mathcal{Z})$ is the smallest aligned box that contains \mathcal{Z} such that the inclusion property holds where $rs(\mathcal{Z})$ is a diagonal matrix whose diagonal elements are $rs(\mathcal{Z})_{ii} = \sum_{j=1}^r \|R_{ij}\|$, for $\forall i \in \mathcal{I}_n$.

Property 3 (Reduction Operator). A reduction operator denoted \downarrow_q permits to reduce the number of generators of a zonotope $\langle c, R \rangle$ to a fixed number q while preserving the inclusion property $\langle c, R \rangle \subset \langle c, \downarrow_q \{R\} \rangle$. A simple yet efficient solution to compute $\downarrow_q \{R\}$ is given in [31]. It consists in sorting the columns of R on decreasing Euclidean norm and enclosing the influence of the smaller columns only into an easily computable interval hull, so that the resulting matrix $\downarrow_q \{R\}$ has no more than q columns.

2.2. Problem Statement

We consider a class of nonlinear systems of the form

$$\begin{aligned} x_{k+1} &= \Psi(x_k, u_k) + E_\omega \omega_k, \\ y_k &= Cx_k + E_v v_k, \end{aligned} \quad (1)$$

with $x \in \mathcal{D}_x$ and $u \in \mathcal{D}_u$. For system (1), $x \in \mathbb{R}^{n_x}$ is the state, $u \in \mathbb{R}^{n_u}$ is the control input, $y \in \mathbb{R}^{n_y}$ is the system output, $\omega \in \mathbb{R}^{n_\omega}$ is the disturbance input, and $v \in \mathbb{R}^{n_v}$ is the process noise. The nonlinear function $\Psi(\cdot) \in \mathbb{R}^{n_x \times n_x}$ is differentiable with respect to the state x . Moreover, the constant matrices C , E_ω and E_v are with appropriate dimensions. Inspired by the TS fuzzy modeling with nonlinear consequents [18, 32], we reformulate system (1) in the form

$$\begin{aligned} x_{k+1} &= A(\xi_k)x_k + \tau(\xi_k, u_k) + G(\xi_k)\phi(x_k, u_k) + E_\omega \omega_k, \\ y_k &= Cx_k + E_v v_k, \end{aligned} \quad (2)$$

For the nonlinear system (2), we assume that the premise variable $\xi_k \in \mathbb{R}^{n_\xi}$ can be measured, i.e., $\xi_k = h(z_k)$ with $h(\cdot) : \mathbb{R}^{n_z} \rightarrow \mathbb{R}^{n_\xi}$ and the vector z_k contains the elements of the output vector y_k , which are not corrupted by the noise v_k . The nonlinear function $\phi(x_k, u_k)$ is differentiable with respect to the state x_k . Note that the matrix-valued functions $A(\xi_k)$ and $G(\xi_k)$, and the vector-valued function $\tau(\xi_k, u_k)$ are measurable, whereas the elements of $\phi(x_k, u_k)$ cannot be measured from the output. Applying the sector nonlinearity approach [14, Chapter 2], the nonlinear system (2) can be *exactly* expressed by r fuzzy IF-THEN rules in the compact set \mathcal{D}_x with local nonlinear consequents [18]:

$$\begin{aligned} \text{RULE } R_i : \quad & \text{IF } \xi_{1k} \text{ is } \mathcal{M}_1^i \text{ and } \dots \text{ and } \xi_{pk} \text{ is } \mathcal{M}_p^i \\ \text{THEN } & \begin{cases} x_{k+1} = A_i x_k + \tau(\xi_k, u_k) + G_i \phi(x_k, u_k) + E_\omega \omega_k \\ y_k = Cx_k + E_v v_k \end{cases} \end{aligned} \quad (3)$$

where (A_i, G_i) are known constant matrices with appropriate dimensions, R_i denotes the i th fuzzy inference rule. \mathcal{M}_j^i , with $i \in \mathcal{I}_r$ and $j \in \mathcal{I}_p$, is the fuzzy set. The fuzzy membership functions are given by

$$h_i(\xi_k) = \frac{\prod_{j=1}^p \mu_j^i(\xi_{jk})}{\sum_{i=1}^r \prod_{j=1}^p \mu_j^i(\xi_{jk})}, \quad \forall i \in \mathcal{I}_r,$$

where $\mu_j^i(\xi_{jk})$ represents the membership grade of ξ_{jk} in the respective fuzzy set \mathcal{M}_j^i . Note that the MFs satisfy the following convex sum property:

$$\sum_{i=1}^r h_i(\xi_k) = 1, \quad 0 \leq h_i(\xi_k) \leq 1, \quad \forall i \in \mathcal{I}_r. \quad (4)$$

Let \mathcal{H} be the set of the membership functions satisfying (4), i.e., $h = [h_1(\xi_k), h_2(\xi_k), \dots, h_r(\xi_k)]^\top \in \mathcal{H}$. Note that $h_+ = [h_1(\xi_{k+1}), h_2(\xi_{k+1}), \dots, h_r(\xi_{k+1})]^\top \in \mathcal{H}$. Using the center-of-gravity method for defuzzification, the TS fuzzy system (3) can be represented in the compact form

$$\begin{aligned} x_{k+1} &= A(h)x_k + \tau(\xi_k, u_k) + G(h)\phi(x_k, u_k) + E_\omega \omega_k \\ y_k &= Cx_k + E_v v_k \end{aligned} \quad (5)$$

where

$$[A(h) \quad G(h)] = \sum_{i=1}^r h_i(\xi_k) [A_i \quad G_i].$$

Remark 1. Note that all the unmeasurable premise variables of system (1) are isolated in the nonlinear term $\phi(x_k, u_k)$ in (5).

The following assumptions are considered for system (5).

Assumption 1. The nonlinear function $\phi(x_k, u_k)$ satisfies the following condition:

$$\underline{\theta}_{ij} \leq \frac{\partial \phi_i}{\partial x_j}(x, u) \leq \bar{\theta}_{ij}, \quad x \in \mathcal{D}_x, \quad u \in \mathcal{D}_u, \quad (6)$$

where

$$\underline{\theta}_{ij} = \min_{\mu \in \mathcal{D}_x \times \mathcal{D}_u} \left(\frac{\partial \phi_i}{\partial x_j}(\mu) \right), \quad \bar{\theta}_{ij} = \max_{\mu \in \mathcal{D}_x \times \mathcal{D}_u} \left(\frac{\partial \phi_i}{\partial x_j}(\mu) \right),$$

for $\forall (i, j) \in \mathcal{I}_{n_\phi} \times \mathcal{I}_{n_x}$.

Assumption 2. The unknown but bounded uncertainties ω_k and v_k belong to the convex and compact sets, defined by the following centered zonotopes:

$$\omega_k \in \mathcal{W} \doteq \langle R_\omega \rangle, \quad v_k \in \mathcal{V} \doteq \langle R_v \rangle, \quad \text{for } k \geq 0, \quad (7)$$

where $R_\omega \in \mathbb{R}^{n_\omega \times n_\omega}$ and $R_v \in \mathbb{R}^{n_v \times n_v}$ are respectively generator matrices of the sets \mathcal{W} and \mathcal{V} .

Assumption 3. The initial state x_0 belongs to the zonotopic set $\mathcal{X}_0 = \langle c_0, R_0 \rangle$, where $c_0 \in \mathbb{R}^{n_x}$ denotes the center and $R_0 \in \mathbb{R}^{n_x \times n_x}$ is the non-empty generator matrix of the initial zonotope \mathcal{X}_0 .

For the estimation of the uncertain nonlinear system (2), we consider the following Luenberger observer structure:

$$\begin{aligned} \hat{x}_{k+1} &= A(h)\hat{x}_k + \pi(\xi_k, \hat{x}_k, u_k) + L(h)(y_k - \hat{y}_k), \\ \hat{y}_k &= C\hat{x}_k, \end{aligned} \quad (8)$$

where $\pi(\xi_k, \hat{x}_k, u_k) = \tau(\xi_k, u_k) + G(h)\phi(\hat{x}_k, u_k)$, \hat{x}_k and \hat{y}_k are respectively the state estimation and the output prediction. The MF-dependent observer gain $L(h) \in \mathbb{R}^{n_x \times n_y}$ is to be designed. Let us define the state estimation error as

$$\tilde{x}_k = x_k - \hat{x}_k. \quad (9)$$

Then, the dynamics of the state estimation error can be obtained from (2) and (8) as follows:

$$\tilde{x}_{k+1} = \hat{A}(h)\tilde{x}_k + G(h)\Delta_\phi + E_\omega \omega_k - L(h)E_v v_k, \quad (10)$$

where

$$\hat{A}(h) = A(h) - L(h)C, \quad \Delta_\phi = \phi(x_k, u_k) - \phi(\hat{x}_k, u_k). \quad (11)$$

The following differential mean value theorem is useful to deal with the mismatching term Δ_ϕ , which has caused a major technical challenge for TS fuzzy observer design [18].

Lemma 1 ([33]). If function $f(x)$ is differentiable on $\text{co}(a, b)$, where $f(x) : \mathbb{R}^{n_x} \rightarrow \mathbb{R}^q$ and $a, b \in \mathbb{R}^{n_x}$, then, there exists constant vectors $s_i \in \text{co}(a, b)$, $s_i \neq a$ and $s_i \neq b$ for $\forall i \in \mathcal{I}_q$, such that

$$f(a) - f(b) = \left(\sum_{i=1}^q \sum_{j=1}^n \mu_q(i) \mu_{n_x}^\top(j) \frac{\partial f_i}{\partial x_j}(s_i) \right) (a - b). \quad (12)$$

Note that the differential mean value theorem has been also exploited in the literature for different TS observer designs [17, 18, 34].

Applying Lemma 1 to the nonlinear function $\phi(x, u)$, there exists a constant vector $\tilde{s}_i \in \text{co}(x, \hat{x})$, for $\forall i \in \mathcal{I}_{n_\phi}$, such that

$$\Delta_\phi = \Phi(\theta) (x - \hat{x}), \quad (13)$$

with

$$\Phi(\theta) = \sum_{i=1}^{n_\phi} \sum_{j=1}^{n_x} \mu_{n_\phi}(i) \mu_{n_x}^\top(j) \theta_{ij}, \quad \theta_{ij} = \frac{\partial \phi_i}{\partial x_j}(\tilde{s}_i, u),$$

for $\forall (i, j) \in \mathcal{I}_{n_\phi} \times \mathcal{I}_{n_x}$. For simplicity, we denote

$$\theta = [\theta_{11}, \dots, \theta_{1n_x}, \dots, \theta_{n_\phi n_x}] \quad (14)$$

Due to the boundedness condition (6), the parameter vector θ belongs to a bounded convex set \mathcal{S}_ϕ , whose the set of $2^{n_\phi n_x}$ vertices is given by

$$\mathcal{V}_\phi = \{\theta = [\theta_{11}, \dots, \theta_{1n_x}, \dots, \theta_{n_\phi n_x}] : \theta_{ij} \in \{\underline{\theta}_{ij}, \bar{\theta}_{ij}\}\}.$$

The state-bounding observer corresponding to the nonlinear system (2) can be obtained as a zonotope $\hat{\mathcal{X}}_k = \langle c_k^x, R_k^x \rangle$ using the Luenberger-type observer (8) and Proposition 1 when bounded uncertainties and set-zonotopic representation are considered.

Proposition 1 (Zonotopic Observer Structure). Consider system (2) with Assumptions 1–3 and the Luenberger observer structure (8). The center c_k^x and shape matrix R_k^x of $\hat{\mathcal{X}}_k$ can be computed recursively as

$$\begin{aligned} c_{k+1}^x &= \hat{A}(h)c_k^x + \tau(\xi_k, u_k) + G(h)\phi(c_k^x, u_k) + L(h)y_k, \\ R_{k+1}^x &= [\hat{A}(h)R_k^x \quad G(h)R_k^\theta \quad E_\omega R_\omega \quad -L(h)E_v R_v], \end{aligned} \quad (15)$$

where $\bar{R}_k^x = \downarrow_q \{\bar{R}_k^x\}$. Moreover, the state inclusion property $x_k \in \langle c_k^x, R_k^x \rangle$ in Property 2 holds for all $k \geq 0$. Furthermore, the matrix R_k^θ indicates the effect of the mismatching nonlinear term Δ_ϕ , whose computational procedure is detailed later in Remark 2.

Proof. Assume $x_k \in \langle c_k^x, R_k^x \rangle$, $\omega_k \in \langle 0, R_\omega \rangle$ and $v_k \in \langle 0, R_v \rangle$, for all $k \geq 0$, where the inclusion property is preserved by using the reduction operator, i.e., $x_k \in \langle c_k^x, \bar{R}_k^x \rangle$. Therefore, the state observer (8) can be formulated using the zonotopic representation as $\hat{x}_{k+1} \in \langle c_{k+1}^x, R_{k+1}^x \rangle$, with

$$\begin{aligned} \langle c_{k+1}^x, R_{k+1}^x \rangle &= \langle \hat{A}(h)c_k^x, \hat{A}(h)\bar{R}_k^x \rangle \oplus \langle L(h)y_k, 0 \rangle \\ &\oplus \langle \tau(\xi_k, u_k), 0 \rangle \oplus \langle G(h)\phi(x_k^x, u_k), G(h)R_k^\theta \rangle \\ &\oplus \langle 0, E_\omega R_\omega \rangle \oplus \langle 0, -L(h)E_v R_v \rangle. \end{aligned} \quad (16)$$

Using the Minkowski sum and Property 1, c_{k+1}^x and R_{k+1}^x in (16) can be expressed as in (15), where the center c_{k+1}^x can be interpreted as a classical punctual state estimate of the unknown state x_k and the shape matrix R_{k+1}^x characterizes the zonotopic enclosure of the classical observation error. \square

Note from the expression (16) that the two terms $\langle L(h)y_k, 0 \rangle$ and $\langle \tau(\xi_k, u_k), 0 \rangle$ have no effect on the generator matrix R_{k+1}^x and only alter the center matrix c_{k+1}^x of the propagating zonotope $\langle c_{k+1}^x, R_{k+1}^x \rangle$. Considering the state estimation error dynamics (10), the zonotopic set bounding the state estimation error can be also recursively obtained as

$$\tilde{x}_{k+1} \in \langle R_{k+1}^{\tilde{x}} \rangle, \quad (17)$$

$$\text{with } R_{k+1}^{\tilde{x}} = [\hat{A}(h)\bar{R}_k^{\tilde{x}} \quad G(h)R_k^{\theta} \quad E_{\omega}R_{\omega} \quad -L(h)E_vR_v].$$

Remark 2. The matrix R_k^{θ} represents the effect of the mismatching nonlinear term Δ_{ϕ} on the estimation error. Note that R_k^{θ} is required to obtain the zonotopic sets $\langle c_k^x, R_k^x \rangle$ and $\langle R_{k+1}^{\tilde{x}} \rangle$. Using the boundedness condition (6) and the zonotope inclusion property, Algorithm 1 provides a procedure to recursively compute R_k^{θ} at each time step k . We denote $[\Phi(\theta)]$ the interval matrix derived from $\Phi(\theta)$ in (13), with $\theta \in \mathcal{S}_{\phi}$, $[\tilde{x}_k]$ the interval vector derived from the upper and lower bounds of each element of the vector \tilde{x}_k , and $\text{product}([\Phi(\theta)], [\tilde{x}_k])$ their interval product.

Algorithm 1 Procedure to compute R_k^{θ}

- 1: **initialization** $\mathcal{X}_0 = \langle c_0, R_0 \rangle$ and $[\Phi(\theta)]$ with $\theta \in \mathcal{S}_{\phi}$
 - 2: **for** $k = 1$: **end do**
 - 3: **compute** $R_k^{\tilde{x}}$
 - 4: **compute** $\tilde{x}_{k(i)} \in [\underline{\tilde{x}}_{k(i)}, \bar{\tilde{x}}_{k(i)}]$, for $i \in \mathcal{I}_{n_x}$ by
 - 5: **compute** $\underline{\tilde{x}}_{k(i)}$ and $\bar{\tilde{x}}_{k(i)}$, with $\tilde{x}_{k(i)} \in [\underline{\tilde{x}}_{k(i)}, \bar{\tilde{x}}_{k(i)}]$, for $i \in \mathcal{I}_{n_x}$, by

$$\underline{\tilde{x}}_{k(i)} = -rs(R_k^{\tilde{x}})_i, \quad \bar{\tilde{x}}_{k(i)} = +rs(R_k^{\tilde{x}})_i$$
 - 6: **compute** $[\mathcal{R}_k^{\theta}] = \text{product}([\Phi(\theta)], [\tilde{x}_k])$
 - 7: **compute** $\diamond(\mathcal{Z}_k) = \langle R_k^{\theta} \rangle$ with $\mathcal{Z}_k = \langle [\mathcal{R}_k^{\theta}] \rangle$ using Property 2
 - 8: **extract** R_k^{θ} from $\diamond(\mathcal{Z}_k)$
 - 9: **end for**
-

The estimation problem is now to design the MF-dependent observer gain $L(h)$ for the state bounding observer (15).

3. Zonotopic Observer Design

This section presents two approaches to design the observer gain. The first approach is based on the minimization of the F -radius of a zonotope whereas an \mathcal{H}_{∞} -based approach is used for the second design.

3.1. Criterion-Based Observer Design

As can be seen from Proposition 1, the zonotopic state-bounding observer (15) is parameterized by means of the MF-dependent observer gain $L(h)$ at each time instant k . According to [30, 31], the size of the state-bounding zonotope $\hat{\mathcal{X}}_k = \langle c_k^x, R_k^x \rangle$ can be minimized via its F -radius. The following theorem provides a method to compute $L(h)$ for this purpose.

Theorem 1. Consider the nonlinear TS fuzzy system (5) and its associated Luenberger-type observer (8). The size of the zonotope defined in (15) can be optimized by using the following observer gain:

$$L(h) = \Psi(h)\Omega_k^{-1}. \quad (18)$$

with

$$\Psi(h) = A(h)\tilde{P}_k C^{\top}, \quad \tilde{P}_k = R_k^x R_k^{x\top}, \\ \Omega_k = C\tilde{P}_k C^{\top} + E_v R_v R_v^{\top} E_v^{\top}.$$

Proof. According to [31], minimizing the F -radius and F_W -radius of a zonotope is equivalent to minimizing the trace of its covariance. Therefore, minimizing the F -radius of the zonotope $\hat{\mathcal{X}}_{k+1} = \langle c_{k+1}^x, R_{k+1}^x \rangle$ defined in (15) is equivalent to minimizing the trace of its covariation $\tilde{P}_{k+1} = R_{k+1}^x R_{k+1}^{x\top}$, i.e.,

$$\mathcal{J} = \|R_{k+1}^x\|_F^2 = \text{tr}(R_{k+1}^x R_{k+1}^{x\top}) = \text{tr}(\tilde{P}_{k+1}), \quad (19)$$

where \mathcal{J} denotes the Frobenius radius and \tilde{P} is the covariance of the zonotope matrix R^x . Similarly, minimizing the F_W -radius of the zonotope $\hat{\mathcal{X}}_{k+1}$ is equivalent to minimizing the criterion, i.e.,

$$\mathcal{J}_W = \|R_{k+1}^x\|_{F,W}^2 = \text{tr}(\tilde{W}\tilde{P}_{k+1}), \quad (20)$$

where \mathcal{J}_W denotes the weighted Frobenius radius and $\tilde{W}\tilde{P}$ is the weighted function covariance of the zonotope matrix R_k^x . Note that \tilde{W} is any positive definite weighting matrix. It follows from (15) that

$$\tilde{P}_{k+1} = (A(h) - L(h)C)\tilde{P}_k(A(h) - L(h)C)^{\top} \\ + Q_G(h) + Q_{\omega} + L(h)Q_v L(h)^{\top}, \quad (21)$$

where $Q_G(h) = G(h)R_k^{\theta}R_k^{\theta\top}G(h)^{\top}$, $Q_{\omega} = E_{\omega}R_{\omega}R_{\omega}^{\top}E_{\omega}^{\top}$ and $Q_v = E_v R_v R_v^{\top} E_v^{\top}$. From (21), the criterion \mathcal{J}_W in (20) can be rewritten as

$$\mathcal{J}_W = \text{tr}(\tilde{W}(A(h) - L(h)C)\tilde{P}_k(A(h) - L(h)C)^{\top} \\ + \tilde{W}Q_G(h) + \tilde{W}Q_{\omega} + \tilde{W}L(h)Q_v L(h)^{\top}). \quad (22)$$

Then, the optimal value of the observer gain $L(h)$ is determined such that $\frac{\partial \mathcal{J}_W}{\partial L(h)} = 0$. Considering (22), this latter yields

$$\partial_{L(h)} \text{tr}(\tilde{W}L(h)(C\tilde{P}_k C^{\top} + Q_v)L(h)^{\top}) \\ - 2\partial_{L(h)} \text{tr}(\tilde{W}A(h)P_k C^{\top} L(h)^{\top}) = 0. \quad (23)$$

Following the same arguments on matrix calculus as in [31], the equality (23) can be rewritten as

$$\Omega_k^{\top} L(h)^{\top} \tilde{W} = C P_k^{\top} A(h)^{\top} \tilde{W}. \quad (24)$$

By right multiplication with \tilde{W}^{-1} and transposition, it follows from (24) that

$$L(h)\Omega_k = A(h)\tilde{P}_k C^\top, \quad (25)$$

which, in turn, leads to the observer gain expression in (18). \square

Remark that the observer gain expression (18) is completely independent to the choice of the weighting matrix $\tilde{W} \succ 0$.

3.2. \mathcal{H}_∞ -Based Observer Design

The key goal when constructing the state-bounding observer is to reduce the influence of unknown uncertainties/disturbances. To this end, we consider the \mathcal{H}_∞ -based technique to design the observer gain $L(h)$ for the zonotopic observer in Proposition 1. The following lemma is useful for \mathcal{H}_∞ observer design.

Lemma 2 (Relaxation Lemma [35]). For $h, h_+ \in \mathcal{H}$, the MF-dependent inequality

$$\sum_{i=1}^r \sum_{j=1}^r \sum_{q=1}^r h_i(\xi_k) h_j(\xi_k) h_q(\xi_{k+1}) \Pi_{ijq} \succ 0,$$

holds if

$$\begin{aligned} \Pi_{ijq} &\succ 0, \quad i \in \mathcal{I}_r, \\ \frac{2}{r-1} \Pi_{iiq} + \Pi_{ijq} + \Pi_{jiq} &\succ 0, \quad i, j, q \in \mathcal{I}_r. \end{aligned} \quad (26)$$

Note that other relaxation results with different degrees of complexity and/or conservatism can be found in [36].

For \mathcal{H}_∞ observer design, the estimation error system (10) is rewritten as follows:

$$\tilde{x}_{k+1} = \hat{A}(h)\tilde{x}_k + \hat{E}(h)d_k, \quad (27)$$

with $d_k = [\Delta_\phi^\top \quad \omega_k^\top \quad v_k^\top]^\top$ and

$$\hat{E}(h) = [G(h) \quad E_\omega \quad -L(h)E_v]. \quad (28)$$

The following theorem presents sufficient conditions to design an TS fuzzy observer gain such that system (27) achieves a pre-defined \mathcal{H}_∞ -gain level.

Theorem 2. Consider the state estimation error dynamics (27) with the output performance vector $z_k = \tilde{x}_k$. If there exist positive definite matrices $P_i \in \mathbb{R}^{n_x \times n_x}$, symmetric matrices $N_i \in \mathbb{R}^{n_x \times n_x}$, matrices $M_i \in \mathbb{R}^{n_x \times n_y}$, for $i \in \mathcal{I}_r$, and a positive scalar γ , such that

$$\Gamma_{iiq} \succ 0, \quad i, q \in \mathcal{I}_r, \quad (29a)$$

$$\frac{2}{r-1} \Gamma_{iiq} + \Gamma_{ijq} + \Gamma_{jiq} \succ 0, \quad i, j, q \in \mathcal{I}_r, \quad i \neq j, \quad (29b)$$

where

$$\Gamma_{ijq} = \begin{bmatrix} P_i - I & \star & \star & \star & \star \\ 0 & \gamma I & \star & \star & \star \\ 0 & 0 & \gamma I & \star & \star \\ 0 & 0 & 0 & \gamma I & \star \\ \Gamma_{ij}^{51} & \Gamma_{ij}^{52} & \Gamma_{ij}^{53} & \Gamma_{ij}^{54} & N_i + N_i^\top - P_q \end{bmatrix},$$

and

$$\begin{aligned} \Gamma_{ij}^{51} &= N_i A_j - M_i C, & \Gamma_{ij}^{52} &= N_i G_j, \\ \Gamma_{ij}^{53} &= N_i E_\omega, & \Gamma_{ij}^{54} &= -M_i E_v. \end{aligned}$$

Then, system (10) is stable with an \mathcal{H}_∞ -gain from d_k to z_k is smaller than $\sqrt{\gamma}$. Moreover, the MF-dependent observer gain can be computed as

$$L(h) = N(h)^{-1} M(h), \quad (30)$$

with $[N(h) \quad M(h)] = \sum_{i=1}^r h_i(\xi_k) [N_i \quad M_i]$.

Proof. Applying the relaxation result in Lemma 2, it follows that condition (29) implies the following inequality:

$$\begin{bmatrix} P(h) - I & \star & \star & \star & \star \\ 0 & \gamma I & \star & \star & \star \\ 0 & 0 & \gamma I & \star & \star \\ 0 & 0 & 0 & \gamma I & \star \\ \Gamma_{51}(h) & \Gamma_{52}(h) & \Gamma_{53}(h) & \Gamma_{54}(h) & \Gamma_{55}(h, h_+) \end{bmatrix} \succ 0, \quad (31)$$

with

$$\begin{aligned} \Gamma_{51}(h) &= N(h)A(h) - M(h)C, \\ \Gamma_{52}(h) &= N(h)G(h), \\ \Gamma_{53}(h) &= N(h)E_\omega, \\ \Gamma_{54}(h) &= -M(h)E_v, \\ \Gamma_{55}(h, h_+) &= N(h) + N(h)^\top - P(h_+), \\ P(h_+) &= \sum_{q=1}^r h_q(\xi_{k+1}) P_q. \end{aligned}$$

Using the definitions of $\hat{A}(h)$ in (11) and $\hat{E}(h)$ in (28), inequality (31) can be rewritten in the following more compact form:

$$\begin{bmatrix} P(h) - I & \star & \star \\ 0 & \gamma I & \star \\ N(h)\hat{A}(h) & N(h)\hat{E}(h) & \Gamma_{55}(h, h_+) \end{bmatrix} \succ 0. \quad (32)$$

Then, pre- and post-multiplying (32) by the following matrix

$$\begin{bmatrix} I & 0 & -\hat{A}(h)^\top \\ 0 & I & -\hat{E}(h)^\top \end{bmatrix}$$

and its transpose, we obtain

$$\begin{bmatrix} \Lambda(h) - P(h) + I & \star \\ \hat{E}(h)^\top P(h_+) \hat{A}(h) & \hat{E}(h)^\top P(h_+) \hat{E}(h) - \gamma I \end{bmatrix} \prec 0, \quad (33)$$

with $\Lambda(h) = \hat{A}(h)^\top P(h_+) \hat{A}(h)$. Pre- and post-multiplying (33) with $[\tilde{x}_k^\top \quad d_k^\top]$ and its transpose, we obtain the following condition after some algebraic manipulations:

$$\Delta V_k + z_k^\top z_k - \gamma d_k^\top d_k < 0, \quad (34)$$

where $\Delta V_k = V(\tilde{x}_{k+1}) - V(\tilde{x}_k)$ is the variation of the fuzzy Lyapunov function candidate $V(\tilde{x}_k) = \tilde{x}_k^\top P(h)\tilde{x}_k$ along the solution of the estimation error system (10). Summing both

sides of inequality (34) from 0 to the T_f -th instant while assuming zero-initial condition, i.e., $x_0 = 0$, we have

$$V(\tilde{x}_{T_f}) + \sum_{k=0}^{T_f} (z_k^\top z_k - \gamma d_k^\top d_k) < 0. \quad (35)$$

Since $V(\tilde{x}_{T_f}) \geq 0$, it follows from (35) that $\|z_k\|_2^2 < \gamma \|d_k\|_2^2$. Then, the \mathcal{H}_∞ -gain of system (10) is less than $\sqrt{\gamma}$. This concludes the proof. \square

Remark 3. Note that a minimization of the \mathcal{H}_∞ -gain performance level $\sqrt{\gamma}$ allows minimizing the effect of uncertain term d_k on the state estimated error \tilde{x}_k . Hence, to achieve the optimal MF-dependent observer gain $L(h)$, we can solve the following LMI-based optimization problem:

$$\min_{(\gamma, P_i, M_i, N_i), i \in \mathcal{I}_r} \gamma, \quad (36)$$

subject to inequalities (29).

Remark 4. The \mathcal{H}_∞ design conditions in Theorem 2 or the optimization problem in (36) are expressed in terms of LMI constraints, which can be efficiently solved with numerical solvers. All the optimization problems in this paper are solved using the YALMIP toolbox [37]. Moreover, all simulations are performed in a PC with CPU of Intel(R) Core(TM) i7-10610U 2.30GHz and 16.0GB memory.

Remark 5. In Sections 3.1 and 3.2, we propose methods to design appropriate observer gains to improve the estimation performance under the effects of uncertainties by reducing the size of the state bounding zonotopes. To this end, the F -radius-based technique is used to compute a criterion-based observer gain in Theorem 1 while the \mathcal{H}_∞ -based technique is exploited to develop the design conditions in Theorem 2. The key difference between Theorems 1 and 2 is as follows. The time-varying criterion-based observer gain (18) is directly computed with an online procedure, which may result in a heavy computational burden because the dimensions of R_k^x in (15) can be quite large. However, with Theorem 2 the decision matrices involved in the observer gain (30) can be computed offline, which can be more appropriate for many real-world settings.

3.3. Application to Fault Detection

For fault detection purposes, we compute the residual signal $r_k = y_k - \hat{y}_k$ as follows:

$$r_k = C\tilde{x}_k + E_v v_k. \quad (37)$$

The logic of fault detection test is based on checking the consistency of the measurements with a fault-free model. Then, considering Proposition 1, the output prediction vector \hat{y}_k in (8) satisfies

$$\hat{y}_k \in \langle c_k^y, R_k^y \rangle = \langle Cc_k^x, C\bar{R}_k^x \rangle \oplus \langle 0, E_v R_v \rangle. \quad (38)$$

Hence, the center and the shape matrix of the obtained zonotope $\hat{Y}_k = \langle c_k^y, R_k^y \rangle$ are respectively given by

$$c_k^y = Cc_k^x, \quad (39a)$$

$$R_k^y = [C\bar{R}_k^x \quad E_v R_v]. \quad (39b)$$

Moreover, since the zonotopic set representation is considered, the bounds of the residual signal r_k in (37) can be also characterized by a zonotope. As a result, the zonotopic set $\mathcal{R}_k = \langle c_k^r, R_k^r \rangle$ of the residual signal r_k of the nonlinear model (2) can be obtained using the observer (8) and Proposition 1 as

$$\begin{aligned} c_k^r &= y_k - Cc_k^x, \\ R_k^r &= [-C\bar{R}_k^x \quad -E_v R_v]. \end{aligned} \quad (40)$$

Then, the fault detection test can be done by checking if $0 \notin \langle c_k^r, R_k^r \rangle$ at each time instant k .

Remark 6. The computational burden can be reduced by checking whether 0 is inside or not an aligned box $\langle c_k^r, b(R_k^r) \rangle$ enclosing the zonotope $\langle c_k^r, R_k^r \rangle$, i.e.,

$$0 \notin \langle c_k^r, b(R_k^r) \rangle, \quad k \in \mathbb{N}, \quad (41)$$

with $b(R_k^r) = \text{diag}(|R_r| \mathbf{1})$, where $|\cdot|$ is the element-by-element absolute value operator, $\mathbf{1}$ is a column vector of ones and $\text{diag}(\cdot)$ returns a diagonal matrix from a vector of diagonal elements [38]. If condition (41) holds, the existence of the fault is detected. Otherwise, the system is considered healthy. Algorithm 2 summarizes the fault detection test procedure using the proposed zonotopic TS observer.

Algorithm 2 Fault detection test using zonotopic observers

- 1: **input:** y_k and $\tau(\xi_k, u_k)$
 - 2: **initialization:** $\mathcal{X}_0 = \langle c_0, R_0 \rangle$ and $[\Phi(\theta)]$ with $\theta \in \mathcal{S}_\phi$
 - 3: **for** $k = 1$: **end do**
 - 4: **compute** R_k^θ
 - 5: **compute** $\hat{X}_k = \langle c_k^x, R_k^x \rangle$,
 - 6: **compute** $\hat{Y}_k = \langle c_k^y, R_k^y \rangle$
 - 7: **compute** $\mathcal{R}_k = \langle c_k^r, R_k^r \rangle$
 - 8: **if** $0 \notin \langle c_k^r, b(R_k^r) \rangle$ **then**
 - 9: $fault \leftarrow true$
 - 10: **else**
 - 11: $fault \leftarrow false$
 - 12: **end if**
 - 13: $k \leftarrow k + 1$
 - 14: **end for**
-

4. Illustrative Results with an Autonomous Vehicle

Hereafter, the effectiveness of the proposed methods for zonotopic observer design is demonstrated an autonomous vehicle application. This example is selected to evaluate the estimation performance obtained with the criterion-based method and the \mathcal{H}_∞ based approach. The results are also compared to the TS fuzzy observer obtained from the previous work [29]. Note that the \mathcal{H}_∞ based approach proposed in this paper is referred to as non-quadratic design whereas the zonotopic observer design in [29] is referred to as quadratic design.

We consider the problem of state estimation and fault detection for an autonomous ground vehicle, whose schematic is

depicted in Figure 1. The vehicle nonlinear dynamics in the horizontal plane can be described as follows [39]:

$$\begin{aligned}\dot{v}_x &= \frac{T_{\text{eng}} - C_x v_x^2}{I_e} + v_y r + F_w, \\ \dot{v}_y &= \frac{F_{yf} + F_{yr} - C_y v_y^2}{M} - v_x r, \\ \dot{r} &= \frac{l_f F_{yf} - l_r F_{yr}}{I_z},\end{aligned}\quad (42)$$

where v_x is the vehicle longitudinal speed, v_y is the lateral speed, r is the vehicle yaw rate, T_{eng} is the torque input for the vehicle longitudinal dynamics, F_{yf} is the cornering forces at the front tires, F_{yr} is the cornering forces at the rear tires, and F_w represents the impact of the longitudinal disturbance force. The vehicle parameters are given in Table 1.

Table 1: Vehicle parameters.

Parameter	Description	Value
M	Vehicle mass	1476 [kg]
l_f	Distance from gravity center to front axle	1.13 [m]
l_r	Distance from gravity center to rear axle	1.49 [m]
I_e	Effective longitudinal inertia	442.8 [kgm ²]
I_z	Vehicle yaw moment of inertia	1810 [kgm ²]
C_f	Front cornering stiffness	57000 [N/rad]
C_r	Rear cornering stiffness	59000 [N/rad]
C_x	Longitudinal aerodynamic drag coefficient	0.35 [-]
C_y	Lateral aerodynamic drag coefficient	0.45 [-]

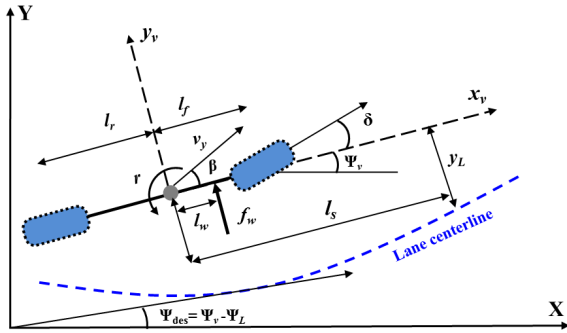


Figure 1: Schematic of a two degrees-of-freedom vehicle model.

Under normal driving conditions with small angle assumption [40, 41], the lateral tire forces F_{yf} and F_{yr} are proportional to the slip angles of each axle. Then, these forces can be approximated as

$$F_{yf} = 2C_f \left(\delta - \frac{v_y - l_f r}{v_x} \right), \quad F_{yr} = 2C_r \left(\frac{l_r r - v_y}{v_x} \right) \quad (43)$$

where δ is the front wheel steering angle. Considering (42) and (43), the nonlinear vehicle dynamics can be described as

$$\begin{aligned}\dot{x} &= A(\xi)x + E_v u + f_v(\xi) + G_v \phi(x) + E_\omega \omega, \\ y &= Cx,\end{aligned}\quad (44)$$

where $x = [v_x \ v_y \ r]^\top$ is the vehicle state vector, $u = [T_{\text{eng}} \ \delta]^\top$ is the control input, $\omega = F_w$ is the disturbance,

and $\phi(x) = v_y^2$ is the unmeasured nonlinearity. The state-space matrices in system (44) are given by

$$\begin{aligned}A(\xi) &= \begin{bmatrix} 0 & r & 0 \\ 0 & -\frac{2(C_f + C_r)}{M v_x} & 0 \\ 0 & \frac{2(l_r C_r - C_f l_f)}{I_z v_x} & 0 \end{bmatrix}, & \xi &= \begin{bmatrix} 1 \\ v_x \\ r \end{bmatrix}, \\ f_v(\xi) &= \begin{bmatrix} -\frac{C_x v_x^2}{I_e} \\ \frac{2(C_r l_r - C_f l_f)}{M v_x} - v_x r \\ -\frac{2(C_f l_f^2 + C_r l_r^2)}{I_z v_x} r \end{bmatrix}, & G_v &= \begin{bmatrix} 0 \\ -\frac{C_y}{M} \\ 0 \end{bmatrix}, \\ E_v &= \begin{bmatrix} \frac{1}{I_e} & 0 \\ 0 & \frac{2C_f}{M} \\ 0 & \frac{2l_f C_f}{I_z} \end{bmatrix}, & E_\omega &= \begin{bmatrix} 1 \\ 0 \\ 0 \end{bmatrix}.\end{aligned}$$

Taking into account the physical limitations during normal driving conditions [41], the compact set of the vehicle state is defined as

$$\mathcal{D}_x = \{v_x \in [\underline{v}_x, \bar{v}_x], v_y \in [\underline{v}_y, \bar{v}_y], r \in [\underline{r}, \bar{r}]\}. \quad (45)$$

where $\underline{v}_x = 5$ [m/s], $\bar{v}_x = 30$ [m/s], $\underline{v}_y = -1.5$ [m/s], $\bar{v}_y = 1.5$ [m/s], $\underline{r} = -0.55$ [rad/s] and $\bar{r} = 0.55$ [rad/s]. For system (44), the vehicle speed v_x and the yaw rate r can be directly measured, which is not the case of the lateral speed v_y . Hence, the output equation is defined as

$$y = Cx, \quad C = \begin{bmatrix} 1 & 0 & 0 \\ 0 & 0 & 1 \end{bmatrix}. \quad (46)$$

The uncertainty ω is assumed unknown but bounded, which belongs to a compact set defined by the following zonotope:

$$\omega \in \mathcal{W} = \langle c_\omega, R_\omega \rangle, \quad (47)$$

where c_ω denotes the center of the set \mathcal{W} with its generator matrix $R_\omega \in \mathbb{R}^{n_\omega \times n_\omega}$. Using the Euler's discretization method with the sampling time $T_s = 0.01$ [s], the discrete-time counterpart of the vehicle model (44) is given by

$$\begin{aligned}x_{k+1} &= A(\xi_k)x_k + E_d u_k + f(\xi_k) + G\phi(x_k) + E_\omega \omega_k, \\ y_k &= Cx_k,\end{aligned}\quad (48)$$

with

$$\begin{aligned}A(\xi_k) &= T_s A_v(\xi_k) + I, & E_d &= T_s E_v, \\ f(\xi_k) &= T_s f_v(\xi_k), & G &= T_s G_v.\end{aligned}$$

Note that $A(\xi) = A(V_x, r)$ with $V_x = \frac{1}{v_x} \in [\underline{V}_x, \bar{V}_x]$. Using the sector nonlinearity approach [14] with the premise vector $\xi_k \in \mathbb{R}^2$, the following four-rule TS fuzzy model of the system (48) can be derived:

$$\begin{aligned}x_{k+1} &= \sum_{i=1}^4 h_i(\xi_k) A_i x_k + E_d u_k + f(\xi_k) + G\phi(x_k) + E_\omega \omega_k, \\ y_k &= Cx_k,\end{aligned}\quad (49)$$

where the local matrices A_i , for $i \in \mathcal{I}_4$, are given by

$$\begin{aligned}A_1 &= A(\underline{V}_x, \underline{r}), & A_2 &= A(\underline{V}_x, \bar{r}), \\ A_3 &= A(\bar{V}_x, \underline{r}), & A_4 &= A(\bar{V}_x, \bar{r}).\end{aligned}$$

The corresponding membership functions $h_i(\xi)$, for $i \in \mathcal{I}_4$, are defined as

$$\begin{aligned} h_1(\xi) &= \Omega_{v_1} \Omega_{r_1}, & h_2(\xi) &= \Omega_{v_1} \Omega_{r_2}, \\ h_3(\xi) &= \Omega_{v_2} \Omega_{r_1}, & h_4(\xi) &= \Omega_{v_2} \Omega_{r_2}, \end{aligned} \quad (50)$$

with

$$\begin{aligned} \Omega_{v_1} &= \frac{\bar{V}_x - V_x}{\bar{V}_x - \underline{V}_x}, & \Omega_{r_1} &= \frac{\bar{r} - r}{\bar{r} - \underline{r}}, \\ \Omega_{v_2} &= \frac{V_x - \underline{V}_x}{\bar{V}_x - \underline{V}_x}, & \Omega_{r_2} &= \frac{r - \underline{r}}{\bar{r} - \underline{r}}. \end{aligned}$$

For illustrations, we consider a driving scenario with the profiles of the engine torque and the steering angle as presented in Figure 2. The state estimation results can be obtained with both the criterion-based approach in Section 3.1 or the \mathcal{H}_∞ approach in Section 3.2. Figure 3 depicts the achieved state estimation result from the system's healthy operating simulation. Note that for the studied model of the autonomous ground vehicle, the minimum feasible solution of γ is found as $\gamma = 0.630$ in the case of the proposed method in Section 3.2. The projection of the computed state-bounding zonotopes into the state space is presented in Figure 4 to make the study of the obtained results easier. As can be seen in Figure 4, when the system is operates in healthy modes, all three different methods can offer a satisfactory estimation performance where the actual values of the states are located inside of the computed upper and lower bounds. Observe also that the non-quadratic design method provide a tighter estimation bounds compared to those of the two other ones. The zonotope $\langle R_k^\theta \rangle$ bounding $\Delta\theta$, computed by Algorithm 1, is illustrated in Figure 5.

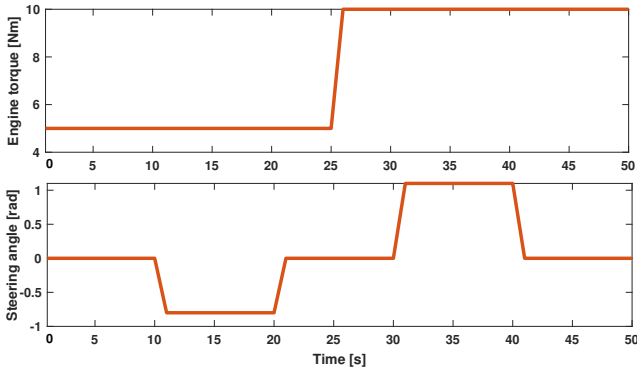


Figure 2: Profiles of the vehicle control inputs.

For the aim of fault detection analysis, the occurrence of an additive step (abrupt) actuator fault is simulated at time instant $k = 15$ and it remains in the system until $k = 30$. The obtained result for the generated residual zonotope and its projection to the residual space are shown in Figures 6 and 7, respectively. As can be seen by looking at the first 15 time instants of the Figure 6, where the system is only affected by the uncertain terms, the observer can properly follow the system using three observer gains and considered threshold (here zero) is inside of the generated zonotopes. But, after fault occurrence at $k = 15$, the zonotopes are affected by the fault and this effect moves the

residual zonotopes, and consequently, existence of fault can be detected since zero is not included within the boundaries. The same point can be seen in Figure 7.

5. Conclusions

This paper has proposed new observer designs for a class of uncertain nonlinear systems represented in TS fuzzy models. As a novelty, the observer gains can be online optimized using the F -radius based technique or offline computed by solving an LMI-based optimization problem derived from \mathcal{H}_∞ filtering technique. In both proposed methods, the influence of all possible uncertain terms and unmeasured premise variables are considered using zonotopic set representation. We also provide a method to take into account the impact of unmeasurable premise variables in the structure of state-bounding observers. The case study section has been used to compare the observer with different gains applied to a autonomous ground vehicle, i.e., when it is solely estimated considering the robustness against uncertainties. Based on the obtained results, the proposed design methods can provide robust observers for a large class of uncertain nonlinear systems. Furthermore, in the presence of faults, the performance of the proposed zonotopic observers is satisfactory. The offline \mathcal{H}_∞ design of observer gains can inspire the real-time implementation of the proposed method into an autonomous ground vehicle available at our laboratory as a future research project. Another promising future work focuses on designing robust TS fuzzy observers while guaranteeing a specified fault sensitivity performance for fault detection purposes, e.g., using multiobjective $\mathcal{H}_\infty/\mathcal{H}_\infty$ specifications with *a priori* information on the finite-frequency of the faults.

Acknowledgment

This work was supported in part by the French Ministry of Higher Education and Research, in part by the National Center for Scientific Research (CNRS), in part by the Hauts-de-France region under the project ELSAT 2020, in part by the ANR Co-CoVeIA project (ANR-19-CE22-0009).

References

- [1] M. Blanke, M. Kinnaert, J. Lunze, M. Staroswiecki, J. Schröder, Diagnosis and Fault-Tolerant Control, Vol. 691, Springer, 2006.
- [2] J. Chen, R. Patton, Robust Model-Based Fault Diagnosis for Dynamic Systems, Vol. 3, Springer Science & Business Media, 2012.
- [3] J. Gertler, Fault detection and isolation using parity relations, Control Eng. Pract. 5 (5) (1997) 653–661.
- [4] M. Basseville, I. Nikiforov, Detection of Abrupt Changes: Theory and Application, Vol. 104, Prentice Hall Englewood Cliffs, 1993.
- [5] R. Kalman, A new approach to linear filtering and prediction problems, J. Basic Eng. 82 (1) (1960) 35–45.
- [6] P. Maybeck, Stochastic Models, Estimation, and Control, Vol. 3, Academic Press, 1982.
- [7] F. Scheppe, Recursive state estimation: Unknown but bounded errors and system inputs, IEEE Trans. Autom. Control 13 (1) (1968) 22–28.
- [8] H. Le, C. Stoica, T. Alamo, E. Camacho, D. Dumur, Zonotopes: From Guaranteed State-Estimation to Control, John Wiley & Sons, 2013.

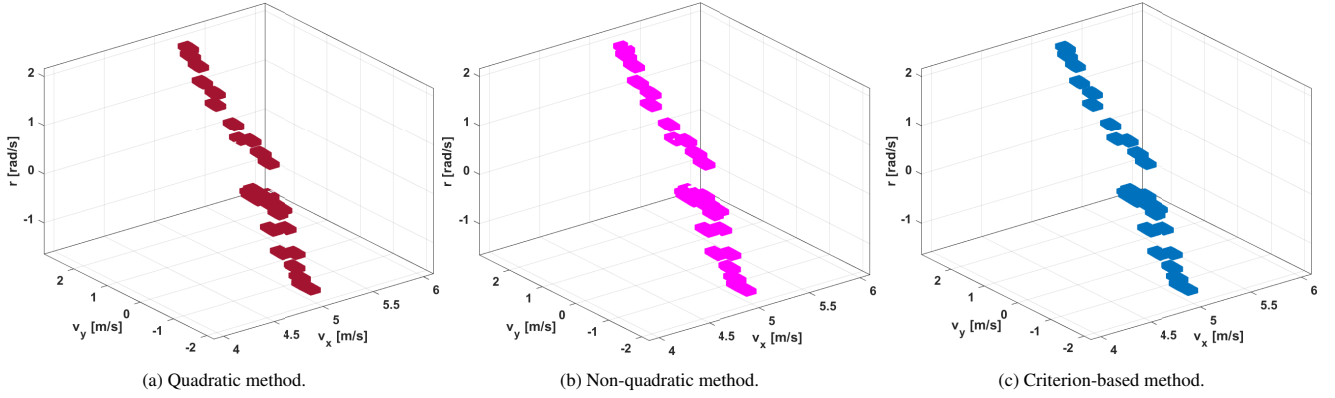


Figure 3: State-bounding zonotopes obtained with three observer design methods.

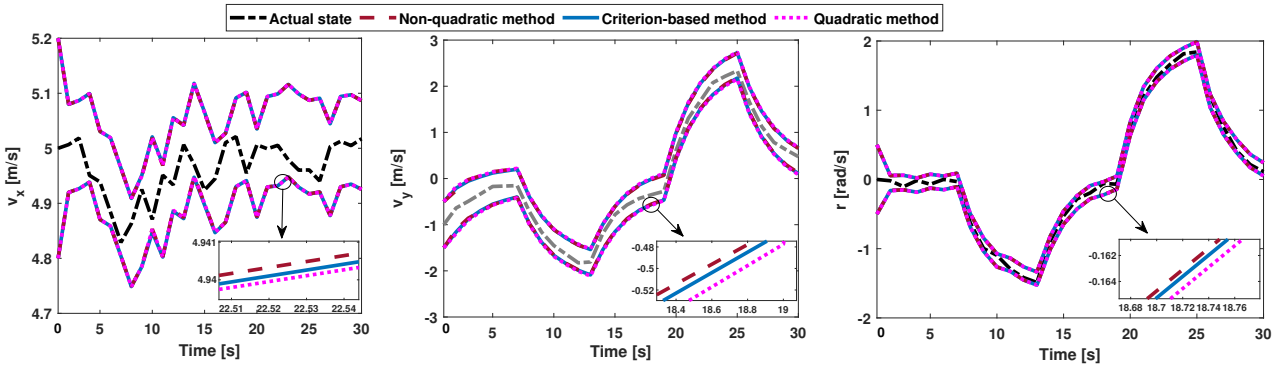


Figure 4: Upper and lower bounds of the state estimation.

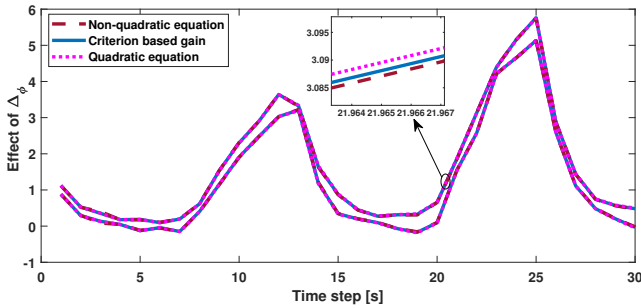


Figure 5: Upper and lower bounds of the zonotope bounding Δ_ϕ .

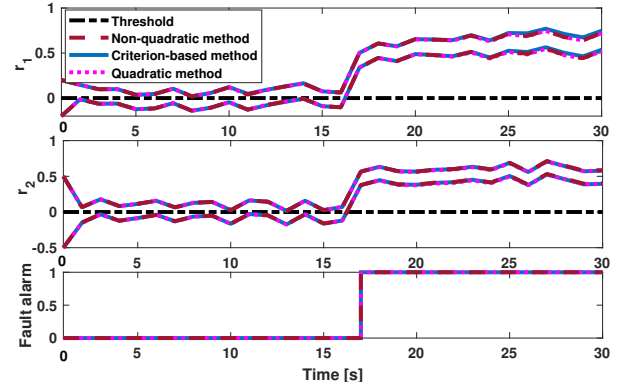


Figure 6: Envelope of the residual in the case of an actuator fault.

- [9] A. Kodakkadan, M. Pourasghar, V. Puig, S. Oлару, C. Ocampo-Martinez, V. Reppa, Observer-based sensor fault detectability: About robust positive invariance approach and residual sensitivity, *IFAC-PapersOnLine* 50 (1) (2017) 5041–5046.
- [10] M. Pourasghar, V. Puig, C. Ocampo-Martinez, Interval observer versus set-membership approaches for fault detection in uncertain systems using zonotopes, *Int. J. Robust Nonlinear Control* 29 (10) (2019) 2819–2843.
- [11] G. Ziegler, Lectures on polytopes (graduate texts in mathematics), *Proc. Edinburgh Mathematical Society* 39 (1) (1996) 189–190.
- [12] W. Kühn, Rigorously computed orbits of dynamical systems without the wrapping effect, *Computing* 61 (1) (1998) 47–67.
- [13] T. Takagi, M. Sugeno, Fuzzy identification of systems and its applications to modeling and control, *IEEE Trans. Syst., Man, Cybern.* (1) (1985) 116–132.
- [14] K. Tanaka, H. Wang, *Fuzzy Control Systems Design and Analysis: a Linear Matrix Inequality Approach*, John Wiley & Sons, 2004.
- [15] A.-T. Nguyen, T. Taniguchi, L. Eciolaza, V. Campos, R. Palhares,

- M. Sugeno, Fuzzy control systems: Past, present and future, *IEEE Comput. Intell. Mag.* 14 (1) (2019) 56–68.
- [16] P. Bergsten, R. Palm, D. Driankov, Observers for Takagi-Sugeno fuzzy systems, *IEEE Trans. Syst., Man, Cybern., Part B (Cybern.)* 32 (1) (2002) 114–121.
- [17] D. Ichalal, B. Marx, S. Mammar, D. Maquin, J. Ragot, How to cope with unmeasurable premise variables in takagi-sugeno observer design: Dynamic extension approach, *Eng. Appl. Artif. Intell.* 67 (2018) 430–435.
- [18] J. Pan, A.-T. Nguyen, T.-M. Guerra, D. Ichalal, A unified framework for asymptotic observer design of fuzzy systems with unmeasurable premise variables, *IEEE Trans. Fuzzy Syst.* 29 (10) (2021) 2938–2948.
- [19] T.-M. Guerra, H. Kerkeni, J. Lauber, L. Vermeiren, An efficient Lyapunov function for discrete T-S models: observer design, *IEEE Trans. Fuzzy Syst.* 20 (1) (2011) 187–192.

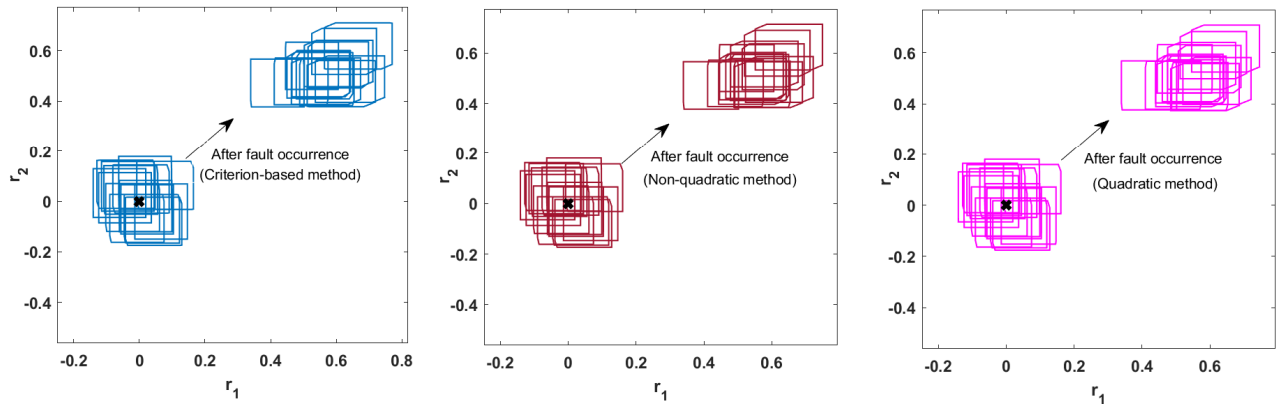


Figure 7: Residual zonotope in the case of actuator fault.

- [20] F. Zhu, Y. Tang, Z. Wang, Interval-observer-based fault detection and isolation design for T-S fuzzy system based on zonotope analysis, *IEEE Trans. Fuzzy Syst.* (2021) 1–doi:10.1109/TFUZZ.2021.3050854.
- [21] Y. Wang, Z. Wang, V. Puig, G. Cembrano, Zonotopic set-membership state estimation for discrete-time descriptor LPV systems, *IEEE Trans. Autom. Control* 64 (5) (2018) 2092–2099.
- [22] M. Zhong, S. Ding, J. Lam, H. Wang, An LMI approach to design robust fault detection filter for uncertain LTI systems, *Automatica* 39 (3) (2003) 543–550.
- [23] M. Pourasghar, C. Combastel, V. Puig, C. Ocampo-Martinez, FD-ZKF: A zonotopic Kalman filter optimizing fault detection rather than state estimation, *J. Process Control* 73 (2019) 89–102.
- [24] Z. Wang, P. Shi, C.-C. Lim, $\mathcal{H}_-/\mathcal{H}_\infty$ fault detection observer in finite frequency domain for linear parameter-varying descriptor systems, *Automatica* 86 (2017) 38–45.
- [25] J. Liu, J. L. Wang, G. H. Yang, An LMI approach to minimum sensitivity analysis with application to fault detection, *Automatica* 41 (11) (2005) 1995–2004.
- [26] D. Henry, Norm-based point of view for fault diagnosis: Application to aerospace missions, *Autom. Control Aerospace* 4 (1) (2011).
- [27] I. Jaimoukha, Z. Li, V. Papakos, A matrix factorization solution to the $\mathcal{H}_-/\mathcal{H}_\infty$ fault detection problem, *Automatica* 42 (11) (2006) 907–912.
- [28] J. Wang, G. Yang, J. Liu, An LMI approach to \mathcal{H}_- index and mixed $\mathcal{H}_-/\mathcal{H}_\infty$ fault detection observer design, *Automatica* 43 (9) (2007) 1656–1665.
- [29] M. Pourasghar, A.-T. Nguyen, T.-M. Guerra, Robust zonotopic observer design: Avoiding unmeasured premise variables for Takagi–Sugeno fuzzy systems, *IFAC-PapersOnLine* 54 (4) (2021) 68–73.
- [30] T. Alamo, J. M. Bravo, E. F. Camacho, Guaranteed state estimation by zonotopes, *Automatica* 41 (6) (2005) 1035–1043.
- [31] C. Combastel, Zonotopes and Kalman observers: Gain optimality under distinct uncertainty paradigms and robust convergence, *Automatica* 55 (2015) 265–273.
- [32] P. Coutinho, R. Araújo, A.-T. Nguyen, R. Palhares, A multiple-parameterization approach for local stabilization of constrained Takagi–Sugeno fuzzy systems with nonlinear consequents, *Inf. Sci.* 506 (2020) 295–307.
- [33] A. Zemouche, M. Boutayeb, I. Bara, Observers for a class of Lipschitz systems with extension to \mathcal{H}_∞ performance analysis, *Syst. Control Lett.* 57 (1) (2008) 18–27.
- [34] A.-T. Nguyen, V. Campos, T.-M. Guerra, J. Pan, W. Xie, Takagi–Sugeno fuzzy observer design for nonlinear descriptor systems with unmeasured premise variables and unknown inputs, *Int. J. Robust Nonlinear Control* 31 (17) (2021) 8353–8372.
- [35] H. Tuan, P. Apkarian, T. Narikiyo, Y. Yamamoto, Parameterized linear matrix inequality techniques in fuzzy control system design, *IEEE Trans. Fuzzy Syst.* 9 (2) (2001) 324–332.
- [36] A. Sala, C. Arino, Asymptotically necessary and sufficient conditions for stability and performance in fuzzy control: Applications of Polya’s theorem, *Fuzzy Sets Syst.* 158 (24) (2007) 2671–2686.
- [37] J. Löfberg, Yalmip: A toolbox for modeling and optimization in Matlab, in: *IEEE Int. Symp. Comput. Aided Control Syst. Des.*, Taipei, 2004, pp. 284–289.
- [38] S.-A. Raka, C. Combastel, Fault detection based on robust adaptive thresholds: A dynamic interval approach, *Annual Rev. Control* 37 (1) (2013) 119–128.
- [39] A.-T. Nguyen, T. Dinh, T.-M. Guerra, J. Pan, Takagi-sugeno fuzzy unknown input observers to estimate nonlinear dynamics of autonomous ground vehicles: Theory and real-time verification, *IEEE/ASME Trans. Mechatron.* 26 (3) (2021) 1328–1338.
- [40] R. Rajamani, *Vehicle Dynamics and Control*, Springer US, 2012.
- [41] A.-T. Nguyen, C. Sentouh, J.-C. Popieul, Driver-automation cooperative approach for shared steering control under multiple system constraints: Design and experiments, *IEEE Trans. Indus. Electron.* 64 (5) (2016) 3819–3830.